

Quantitative evaluation of magnetized plasma based on dis-alignment by laser-induced fluorescence

Roman Bergert, Slobodan Mitic, Markus H. Thoma

Institute of Experimental Physics I, Justus-Liebig-University Giessen
Heinrich-Buff-Ring 16, D-35392 Giessen, Germany

E-mail: Roman.Bergert@physik.uni-giessen.de

Abstract. Quantitative evaluation of tunable laser induced fluorescence (TDLIF) measurements in magnetized plasma accounting for Zeeman splitting of energetic levels and intra-multiplet mixing defining the density distribution (alignment) of excited $2p_8$ multiplet are discussed. TDLIF measurements were used to evaluate light-transport properties in a strongly magnetized optically thick argon plasma under different pressure conditions. Therefore, a system of rate balance equations were constructed to describe optical pumping of individual magnetic sub-levels of $2p_8$ state through frequency separated sub-transitions originating from $1s_4$ magnetic sub-levels.

The density of each $2p_8$ multiplet was described by balancing laser pumping with radiative decay and including additional transitions of excitation between the multiplets driven by neutral collisions. Resulting $2p_8$ magnetic sub-level densities were then further used to model polarization dependent intensities, accounting for self-absorption, and were further compared with measured polarization resolved TDLIF measurements. This enables to obtain unique solutions for the $1s_4$ and $1s_5$ magnetic sub-level densities which were in good agreement with the densities estimated by laser absorption measurements and previous work. The presented method and results can help to understand optical emission between $2p$ and $1s$ states of argon for a magnetized plasma and TDLIF intensity interpretation retrieving magnetic sub-level densities of different $1s$ states.

Keywords: magnetized plasma diagnostics, plasma jet, dielectric barrier discharge (DBD), low-pressure plasma, laser-induced absorption spectroscopy (LAS), magnetized plasma, magnetic sub-level population, argon plasma, laser-induced fluorescence (LIF)

1. Introduction

Influence of an external magnetic field B changes the plasma behavior by influencing movement of a charged particles by the Lorentz force and changing an energetic structure of a plasma components by the Zeeman effect [1] which overall influence the plasma properties. The presence of an external magnetic field in plasma induces anisotropy in motion of a charged particles by reducing cross-field diffusion, while also inducing strong anisotropy in plasma optical emission spectra. Total emitted line intensity is therefore artificial constructed of two polarized components orientated parallel (π -component) or perpendicular ($\sigma\pm$ -component) to the magnetic field vector. Due to such complex effects of magnetic field on plasma components, standard (non-magnetized) description of plasma emission spectra and light transport properties are not suitable. The complexity of optical properties mainly comes from the splitting of an energy levels. The total angular momentum quantum number J of an energetic level will result in $2J+1$ magnetic sub-levels m in the presence of a magnetic field compared to the one single level without a magnetic field. This changes the emission into a system of sub-transitions symmetrically redistributed around the initial unshifted line center. As a result, each spectral transition will have to be rewritten as a sum of optically allowed transitions between corresponding upper and lower magnetic sub-levels [2]. The degeneracy of the levels vanishes under higher external magnetic fields so that an individual description of transitions between magnetic sub-levels is necessary [3]. In optically thick plasma, density distribution of 1s sub-states should be taken into account for correct description of the self-absorption effect and thus the light transport [4].

Description of polarized plasma spectroscopy has been introduced by Fujimoto and colleagues [3, 5, 6, 7] who presented a population-alignment collisional-radiative model (PACRM) based on collisional and radiative interactions between the multiplets and intra-multiplet transitions. Such approach has been demonstrated on the experiments where polarization of plasma optical emission spectroscopy (OES) was induced by highly anisotropic electron energy distribution function (electron beam), mostly in helium or hydrogen, while only limited number of reports considered argon. Also such description is highly non-trivial accounting for less available collisional cross-sections between different multiplets (ground, 1s and 2p states). The possibilities of PACRM for helium has been demonstrated in articles deducing highly interesting plasma properties, such as an anisotropy in the electron energy distribution function based on the modelling of the polarities of a plasma emission lines [8, 9].

The main goal of this work is to evaluate optical emission properties in magnetized argon plasma accounting for Zeeman splitting of radiating ($2p_8$) and 1s stats, density distribution between magnetic sub-levels (alignment) and polarization of plasma emission. Therefore, laser absorption spectroscopy (LAS) and laser induced fluorescence (LIF) were used as diagnostic tools. Description of LAS and evaluation of argon $1s_4$ and $1s_5$ sub-level state densities has been introduced in recent article [4]. Based on the sub-level densities the self-absorption (SA) for different sub-transitions was

discussed. Selfabsorption was included in the interpretation of linear polarized and circular polarized TDLIF at 842 nm and 801 nm. Optical sub-transitions between $1s_4$ and $2p_8$ sub-states were used to pump different magnetic sub-level of $2p_8$.

A model describing the polarization dependent fluorescence was developed including self-absorption and sub-level mixing (dis-alignment) due to neutral collisions which strongly influence the ratio between the two polarities of the fluorescence spectral lines. Such effect changes the description of 2p state densities by introducing disalignment as additional production and losses mechanism competing with radiative decay. The correct analytical description will result in quite strong coupling between involved states densities through dis-alignment and self-absortion so that LIF measurements can be uniquely quantitatively solved resulting in estimations of the 1s magnetic sub-levels densities and dis-alignment constant. The dis-alignment constant has been estimated in [10] where in the presence of weak magnetic field, time dependent polarized LIF measurements has been modeled. However, in most of such experiments, broad and powerful lasers were used for inducing excitation followed by modeling of polarized emission. Another interesting aspect of dis-alignment constant is the temperature dependence which can cause quite opposite effect depending on the quenching atoms [10, 11]. In presented case krypton atoms reduced dis-aligment with temperature increase while for helium, neon and argon dis-alignment constant was increased. Such findings are illustrating the complexity of the effect and quite interesting non-linear response of different argon 2p levels. Although such unique optical properties for magnetized plasma conditions has been investigated since 1960's using highly complicated PACRM formalism, strong and clearly visible effect of neutral gas density on plasma spectra and its practical applications has been purely conveyed to the plasma spectroscopy audience. Therefore we present a model for the quantitative evaluation of LIF measurements using tunable diode laser, carried out on an compact dielectric barrier discharge low pressure plasma in the presence of an external magnetic field of 0.3 T.

2. Methods

Correct interpretation of optical transitions (absorption and induced fluorescence) in magnetized plasma conditions is based on line splitting formalism due to Zeeman effect (resulting in polarization) and its further implications in light transport properties in optically thick conditions. Direct detection of individual induced fluorescence profiles were done with a spectrometer, where a slow laser scan over a broad frequency range was used for pumping frequency shifted sub-transitions. Additionally laser absorption spectroscopy of the $1s_4$ state was used as a reference for the sub-level densities evaluated from TDLIF model.

Under the influence of the magnetic field each energetic level will split into the $2J+1$ multiplet producing system of transitions described by the transition rules. In a strong magnetic field sub-transitions will be shifted in frequency producing absorption

structure symmetric around an-shifted line center. The observed energetic structure and system of transitions of 801 and 842 nm in argon are represented by Kastler diagram as shown in 1. The allowed electric dipole transitions originating from $2p_8$ to $1s_4$ and $1s_5$ are shown by their polarization. The $2p_8$ state splits into 5 sub-levels and same is valid for $1s_5$. Hence 12 different electric dipole transitions are formed ($4 \sigma+$, 4π and $4 \sigma-$), indicated with red arrows between the sub-levels of $2p_8$ and $1s_5$. Nine sub-transitions can be found between $2p_8$ and $1s_4$ ($3 \sigma+$, 3π and $3 \sigma-$) indicated with blue arrows in figure 1.

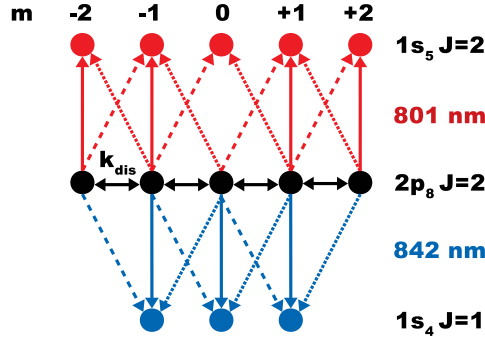


Figure 1. Kastler diagram indicating possible optical transitions π solid lines, $\sigma-$ dashed lines and $\sigma+$ dotted lines from 801 nm in red and 842 nm in blue. Additionally the level-mixing, representing k_{dis} , between the neighbour sub-levels of $2p_8$ is indicated with solid black arrows.

2.1. Tunable diode laser absorption spectroscopy

The description of LAS, polarization dependent sub-level transitions and resulting self-absorption has been described in our previous work [4] and it will be used as a basis for LIF interpretation. Therefore just a short overview will be given on LAS and description of magnetic sub-transitions rates since this has direct impact on optical properties like self-absorption and light transport. Based on the reconstructed absorption profile of individual sub-transition $\kappa(\nu)$ the magnetic sub-level density n_{mj} of targeted 1s states can be calculated according to:

$$n_{mj} = \frac{8\pi}{c^2} \frac{\nu_{m_i, m_j}^2}{A_{J_i, J_j, m_i, m_j}} \kappa(\nu) \quad (1)$$

where c describes the vacuum speed of light, ν_{m_i, m_j} is a central wavelength of the (shifted) transition dependent on the external magnetic field strength, and the Einstein coefficient of transition A_{J_i, J_j, m_i, m_j} between upper $2p_8$ m_i and lower $1s_4$ or $1s_5$ magnetic sub-level states m_j . The expression for the Einstein coefficients describing transitions between upper and lower magnetic sub-levels can be written as [12, 13]:

$$A_{J_i, J_j, m_i, m_j} = (2J_i + 1) A_{ij} \times W$$

$$W = \left| \begin{pmatrix} J_j & q & J_i \\ -m_j & \Delta m_{j,i} & m_i \end{pmatrix} \right|^2 \quad (2)$$

where W represents the Wigner 3-j coefficient to the power of two with the multi-polarity of the transition q equivalent to 1 for electrical dipole transitions, and difference in the magnetic quantum number of the transition $\Delta m_{j,i} = m_j - m_i$. A_{ij} describes the Einstein coefficient (life time) for spontaneous decay of the observed emission in unmagnetized case.

2.2. Tunable diode laser induced fluorescence in magnetized plasma

The laser induced fluorescence measurements were based on same laser excitation scheme consecutively pumping different $2p_8$ sub-levels through 842 nm sub-transitions separated by frequency. The efficiency of laser pumping was therefore proportional to the laser intensity, density of the targeted $1s_4$ m_j -multiplet and Einstein coefficient of sub-transition. Each transition interacts only with corresponding polarity from the an-polarized pumping laser so that laser intensities for different polarization should scale as $I_\pi = 2I_\sigma$.

Pumping of an individual $2p_8$ sub-level would lead to fluorescence of the light emission with polarization determined by the ratio of Einstein coefficients of π and σ component originating from the pumped level and corrected for self-absorption.

However under the observed conditions (magnetically separated transitions) it is evident that the polarization of the induced fluorescence is strongly effected by an additional process leading to appearance of an additional intensities, changing the expected polarization of the fluorescence, which in some cases could not be described by the transition rules. The observed deviations from the predicted polarization are described by inter-multiplet state density mixing driven by collision with neutrals. Such effect would try to equalize the density distribution within multiplets and destroy the alignment. The dis-alignment effect should be consider as an additional production and loss mechanism in the rate balance equation describing $2p_8$ sub-state densities induced by laser pumping.

Measured intensities were corrected by subtracting plasma emission accounting for polarization. Due to the optical selection rules there are no allowed electric dipole π transitions for $m_i = 2$ to $m_j = 2$ of the $2p_8$ to $1s_4$ system and $m_i = 0$ to $m_j = 0$ of the $2p_8$ to $1s_5$ system. Nevertheless the signals were very strong when observing this systems especially when pumping $m_i = 2$ and measuring π fluorescence of 842 nm. This intensities raise with higher pressure indicating the role of level mixing by neutral atoms. Such effect would transfer population from laser pumped level ($m_j = 2$) to other magnetic sub-levels resulting in polarization of light emission determined by final density distribution achieved among magnetic sub-levels. The resulting dis-alignment constants for different 2p states of argon are discussed in [11, 14, 15].

3. Experimental Setup

The experimental setup and discharge configuration is presented in figure 2 with indicated laser path (red arrow) and line of sight for LIF detection (blue arrow). A

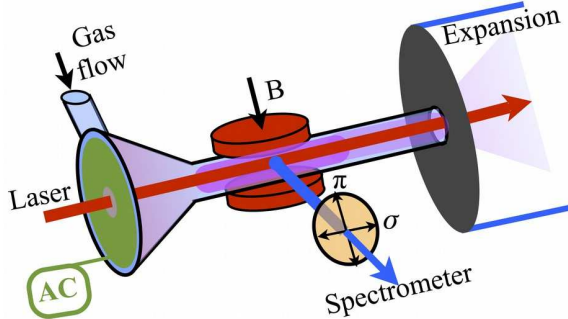


Figure 2. Schematic representation of the experimental setup.

cone shaped glass discharge chamber followed by a tube of 4 mm inner diameter were used to create a compact plasma jet. Open end of the tube was attached to 500 mm long expansion chamber with the vacuum system attached at the end. Driven electrode made of aluminum tape was attached from the outside of the cone base with an opening in the center to introduce a laser beam in axial direction.

A base pressure of 1.4×10^{-1} Pa could be reached. The minimum working pressure inside the tube was estimated to be around 50 Pa at 0.014 slpm gas flow and highest 473 Pa at 0.32 slpm. The working pressure inside the tube was estimated based on the measured Doppler shift in the gas velocity distribution function caused by the induced gas flow through the plasma jet similar as in [16, 17]. The particle velocity, extracted from Doppler shift measurements, can be correlated to the pressure inside the jet through the conservation of volume flow through the jet accounting for the cross-section of the tube and temperature of the gas. The Doppler shift was measured in fluorescence mode using axial laser excitation, along the gas flow, and radial fluorescence measurements at the point between the magnets. The fluorescence signal was detected by photo-diode and recorded together with Fabry-Pérot signal for scale and reference. The intensity of the shift was estimated by comparing with the position of an-shifted radial laser absorption measurements.

Plasma was created by an-bipolar 30 kHz sinusoidal high voltage ($V_{pp} \approx 4$ kV) signal. The external magnetic field was introduced by two cylindrical permanent magnets of 6 mm in diameter inducing a magnetic field of 0.3 T. The field strength was confirmed by a gaussmeter. The magnets were mounted perpendicular to the line of sight at the opposite sides at the discharge tube.

Laser absorption measurements were done in radial direction crossing the tube at position between the magnets, including common optical elements like argon reference cell and a Fabry-Pérot interferometer to monitor laser scanning range and quality. Absorption at 842.47 nm transition was scanned by *TOPTICA DLC 100* laser. A

system of collimators and multimode $200\text{ }\mu\text{m}$ optical fiber was used to manipulate the laser beams, producing an unpolarized probing laser light. A band pass filters at 840 nm with a full width at half-maximum of 10 nm were used in order to suppress the rest of the plasma emission. The absorption measurements were done using optics crossing the tube in radial direction in orientation perpendicular to the magnetic field lines allowing to probe all polarization transitions.

For fluorescence measurements laser light was introduced perpendicular to the external magnetic field in axial direction of the discharge tube along the gas flow. The 3π and $3\sigma+$ transitions of $1s_4$ at 842 nm were used to pump the $2p_8$ sub-levels. Laser scan was set at low scanning frequency allowing to measure simultaneously the induced fluorescence with a high sampling rate (10 ms integration time) using $200\text{ }\mu\text{m}$ optical fiber and a collimator connected to Ocean Optics (USB2000+) spectrometer. The fluorescence was observed perpendicular to the illumination laser using identical optics from the LAS measurements. A linear polarization filter from Thorlabs GmbH with a total transmission of 40 % for unpolarized light was used between the plasma and collection optics to isolate desired polarization from the induced fluorescence. With linear polarization filter oriented parallel to the magnetic field lines only π transitions could be transmitted while perpendicular orientation would transmit only σ . Polarization filter was not completely isolating desired polarity so that 3 % transmissions of the opposite polarity was measured which was further taken into account for correct reconstruction of polarization dependent intensity. Relative sensitivity for linear and circular polarized light was evaluated to 1:0.7, which is usually dependent on an optics and detector system. Such difference in sensitivity of the two polarities was found to be between 0.581 to 0.67 in other studies [10, 18, 19].

4. Results and Discussion

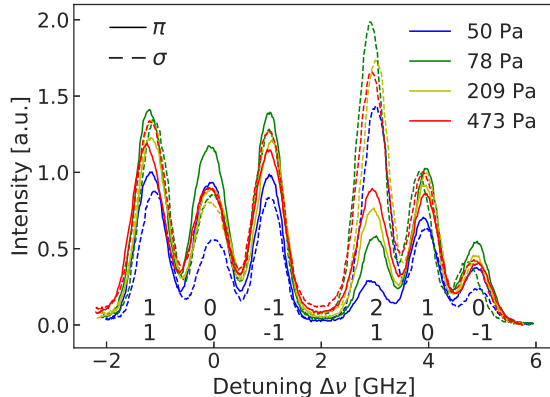


Figure 3. Pressure dependency of $1s_4$ measured fluorescence for four different pressures. Fourth peak of the π profile shows the crucial intensity behaviour due to the dis-alignment effect.

Fluorescence emission recorded at 842 nm branch for 4 different gas pressures are presented in figure 3 colour-coded with thick lines for π and dashed for σ component. The magnetic sub-level quantum number of the involved transitions are indicated at the bottom of the figure with the respective upper and lower magnetic quantum number. The relative changes of the intensities with pressure are noticeable for each polarization component and induced transition. The intensity of not allowed π component originating at A21 transition is clearly visible demonstrating the influence of the dis-alignment on the light transport properties in magnetized plasma.

Systematic changes in polarization of the fluorescence induced at $m_j = -1$ to $m_i = -1$ and $m_j = 1$ to $m_i = 2$ sub-transitions are better presented in figure 4 with intensities scaled by the intensity of the respective $m_i = -1$ to $m_j = -1$ π peak at each pressure. From such representation it is evident that π component only slightly changes the shape with pressure increase for all except $m_i = 2$ to $m_j = 1$ transition which should be pure sigma by the optical selection rules for electrical dipole transitions.

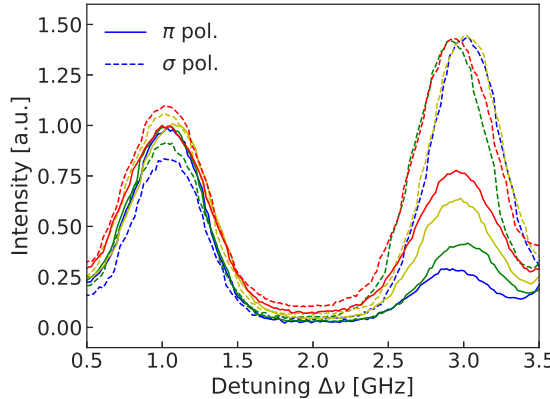


Figure 4. Pressure dependency of $1s_4$ fluorescence for four different pressure same as in figure 3. Peaks were normalized to the left π transition for each pressure originates through pumping of $m_j = -1$ to $m_i = -1$.

Considering the mentioned Kastler diagram (figure 1) and possible transitions it is evident that excitation of different $2p_8$ multiplet ($m_i = -2, -1, \dots, 2$) will produce unique ratio of π to σ fluorescence components for both 842 nm and 801 nm branches. Furthermore optical pumping of $2p_8$ $m_i = \pm 2$ is only possible by sigma polarized component from $1s_4$ $m_j = \pm 1$ and according to the optical selection rules for electrical dipole transitions only sigma polarized light at 842 nm branch should be emitted. However, from the presented measurements the π component detected by the excitation of $m_i = 2$ sub-level state is clearly visible and rather strong with systematic dependence on pressure. This is a solid evidence of the dis-alignment process or intra-multiplet density mixing driven by collisions with the neutral atoms. Such effect would transfer population from the laser pumped sub-level ($m_i = 2$) to other magnetic sub-levels and vice-versa producing a light emission with polarization determined by the final density distribution achieved within the multiplet called alignment. Such effect is also

responsible for detection of π component on 801 nm line when $2p_8\ m_i = 0$ state is optically pumped.

Measured fluorescence was first analyzed by identifying the positions and width of the transitions from measured fluorescence structure, that should be quite similar to the LAS structure analysed in our previous work [4]. In order to model measured fluorescence rate balance equation describing $2p_8$ sub-levels density distribution induced by laser pumping would have to be constructed including radiative decay, dis-alignment effect and self-absorption. In a steady state solution density each of $2p_8$ multiplet can be described in following form:

$$n_{2p_8,m_i} = \frac{I_{\pi/\sigma} A_{J_i J_j, m_i m_j}^{842\text{ nm}} n_{1s_4, m_j} + N k_{\text{dis}} \sum_{a \neq i} n_{2p_8, m_a}}{\sum \left(A_{J_i J_j, m_i m_j}^{842\text{ nm}} \gamma_{m_i, m_j} (n_{1s_4, m_j}) + A_{J_i J_j, m_i m_j}^{801\text{ nm}} \gamma_{m_i, m_j} (n_{1s_5, m_j}) \right) + N k_{\text{dis}}} \quad (3)$$

The $I_{\pi/\sigma}$ describes either the linear or circular polarized laser intensity, N the number of neutral atoms, $A_{J_i J_j, m_i m_j}$ the Einstein coefficient between magnetic sub-levels states (2) and γ_{m_i, m_j} the self-absorption coefficient for the sub-level state m_j . The self-absorption coefficient is dependent on the magnetic sub-level density n_{1s, m_j} and the absorption coefficient. If a sub-state is not directly pumped than the fist factor in numerator in equation 3 describing laser pumping should be neglected.

Rate balance equation accounts the laser pumping as a source of population proportional to Einstein coefficient and targeted 1s sub-level density while additional production due to dis-alignment is included by transfer from neighboring sub-levels described with rate constant k_{dis} in cm^3/s . Here are meant all $2p_8$ sub-levels and not only the direct neighboring what figure 1 shows for simplicity. Same effect is also accounted as a loss mechanism competing with radiation (expressed as effective lifetime) in depopulation of described state. The rate balance equation for each $2p_8$ multiplet will produce closed system of equation that can be solved providing relative density distribution between sub-levels as a result of the laser pumping. The system of equation can be build for each pumped transition providing laser-induced alignment of $2p_8$ state that can be further used to model the intensity of the fluorescence. Here it should be mentioned that the solution of $2p_8, m_i$ is valid for the case when $N k_{\text{dis}} < \sum A_{J_i J_j, m_i m_j}^\lambda$.

Solved sub-level densities for a specific pressure and so specific $N k_{\text{dis}}$ were further used to describe both polarities emitted due to the laser pumping in a following form for 842 nm branch:

$$\begin{aligned} I_\pi^{842\text{ nm}} &= n_{2p_8, 0} A_{0,0}^{842\text{ nm}} \gamma_{0,0} (n_{1s_4, 0}) + 2n_{2p_8, 1} A_{1,1}^{842\text{ nm}} \gamma_{1,1} (n_{1s_4, 1}) \\ I_\sigma^{842\text{ nm}} &= 2n_{2p_8, 0} A_{0,1}^{842\text{ nm}} \gamma_{0,1} (n_{1s_4, 1}) + 2n_{2p_8, 1} A_{1,0}^{842\text{ nm}} \gamma_{1,0} (n_{1s_4, 0}) \\ &\quad + 2n_{2p_8, 2} A_{2,1}^{842\text{ nm}} \gamma_{2,1} (n_{1s_4, 1}) \end{aligned} \quad (4)$$

and for 801 nm branch:

$$\begin{aligned} I_{\pi}^{801 \text{ nm}} &= 2n_{2p_8,1}A_{1,1}^{801 \text{ nm}}\gamma_{1,1}(n_{1s_5,1}) + 2n_{2p_8,0}A_{2,2}^{801 \text{ nm}}\gamma_{2,2}(n_{1s_5,2}) \\ I_{\sigma}^{801 \text{ nm}} &= 2n_{2p_8,0}A_{0,1}^{801 \text{ nm}}\gamma_{0,1}(n_{1s_5,1}) + 2n_{2p_8,1}A_{1,0}^{801 \text{ nm}}\gamma_{1,0}(n_{1s_5,0}) \\ &+ 2n_{2p_8,2}A_{2,1}^{801 \text{ nm}}\gamma_{2,1}(n_{1s_5,1}) + 2n_{2p_8,1}A_{1,2}^{801 \text{ nm}}\gamma_{1,2}(n_{1s_5,2}) \end{aligned} \quad (5)$$

As a result ratios of π to σ for all peaks and each branch could be constructed and further used in comparison with measurements. Some example for 842 nm branch and 801 nm branch for two pressure is shown in figure 5 and 6. Equations constructed for pumping of each of $2p_8$ magnetic sub-level ($m_i = -2, -1, 0, 1, 2$) will create a system of 6 equations with 6 variables ($n_{1s_4, m_j=0}, n_{1s_4, m_j=1}, n_{1s_5, m_j=0}, n_{1s_5, m_j=1}, n_{1s_5, m_j=2}$ and k_{dis}) assuming symmetry in the self-alignment ($n_{-m_j} = n_{m_j}$). The symmetry is confirmed by LAS in this and also in the previous work [4]. The system of equations will result in numerical solutions of $1s_4$ and $1s_5$ multiplet densities and the dis-alignment rate in form $Nk_{\text{dis}} = c_{\text{dis}}$. Here should be emphasized that since only the ratios between the two polarities for each branch were considered in evaluation, there is no need for intensity calibration of the detection system for the two observed wavelengths. This description provides full quantitative evaluation of LIF measurements in magnetized plasma independent on calibration. The quality of the fits is clearly visible from the presented example where besides the reconstructed profiles, relative changes in the intensities between two different pressures could also be reliably reproduced. Similar quality of the fits is achieved for all measured pressure settings. Measured fluorescence intensities and their fits at two different pressures (red low and blue medium pressure) are presented in figure 5 for 842 nm and figure 6 for 801 nm branch. In most cases the deviation is not larger then few percent making this analysis highly efficient.

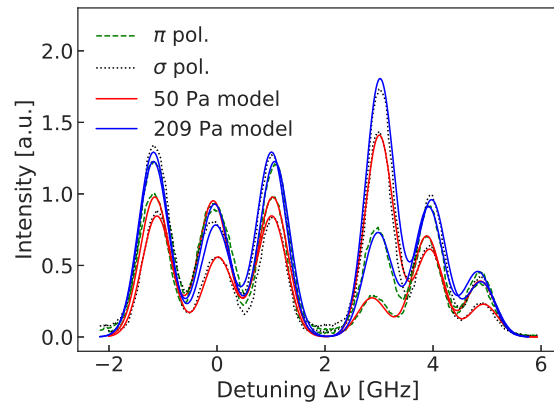


Figure 5. Model and measurements comparison of 842 nm fluorescence for two different pressures and each polarization component.

Reconstructed $1s_4$ and $1s_5$ multiplets densities are presented in figures 7 and 8 respectively, for series of different pressures as indicated on the vertical axis with the

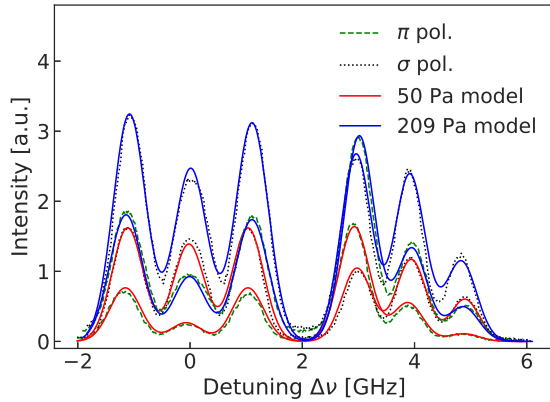


Figure 6. Model and measurements comparison of 801 nm fluorescence for two different pressures and each polarization component.

effective disalignment rate c_{dis} .

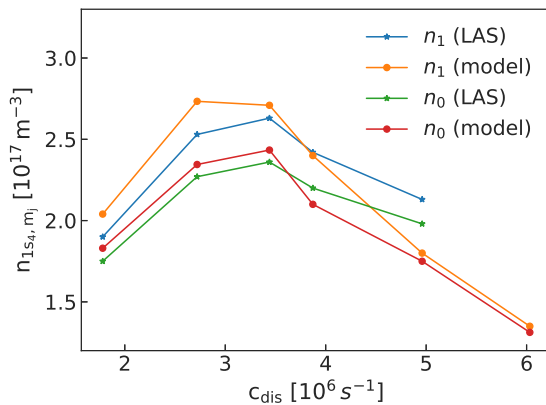


Figure 7. Sub-level density of $1s_4$ measured by LAS and modeled values for different dis-alignment strength c_{dis} (\propto pressure).

The estimated $1s_4$ densities were further compared with the results from direct laser absorption measurements. The estimated densities by this two independent methods are in close agreement accounting for the complexity of the measurements and the evaluation. Alignment between the magnetic sub-levels has been also successfully reconstructed for both states. Reconstructed $1s_5$ multiplet densities can be indirectly compared with the results from the LAS measurements presented in [4] where similar densities and identical negative alignment was observed under very similar conditions.

The pressure at the measurement point (between the magnets) evaluated for used gas flow conditions was estimated to be in range between 50 and 470 Pa. The estimated pressures by LIF were in between the values measured at the extraction side (lower pressure) and in gas flow line (higher pressure), closer to the high pressure side. Based on the pressure estimations the dis-alignment rate coefficient k_{dis} was estimated to be

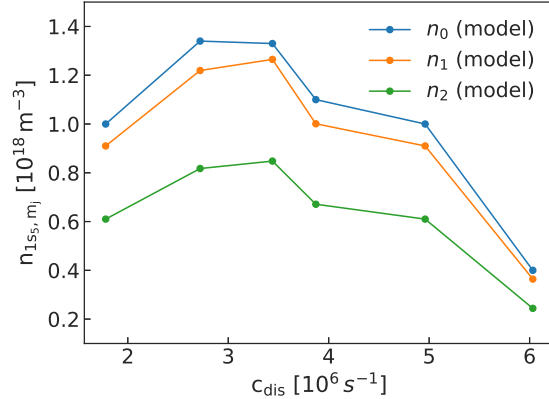


Figure 8. Sub-level density of 1s₅ modeled for different disalignment rate c_{dis} (\propto pressure).

in the range from 0.6 to $1.7 \cdot 10^{-10} \frac{\text{cm}^3}{\text{s}}$ as presented in figure 9. The estimated values at different pressures are not consistent and significantly lower then $14.5 \cdot 10^{-10} \frac{\text{cm}^3}{\text{s}}$ which is reported in [15] although evaluated at higher temperature of 380 K and by a different method. Evaluated temperature of 340 K by LAS in our conditions is lower which could reduce the dis-alignment coefficient according to the temperature dependency reported in [11]. The deviation in estimated rate coefficient at different pressures could be result of pure estimation of pressure inside the tube based on measurements of relatively small shifts (of about 50 MHz) and robust model for pressure estimation. Difference of almost one order of magnitude from reported value at 380 K could be explained as an combined effect of difference in temperature and pressure range, pure pressure estimations and different measurement methods. Another possibility is that with our model an effective dis-alignment rate coefficient is estimated.

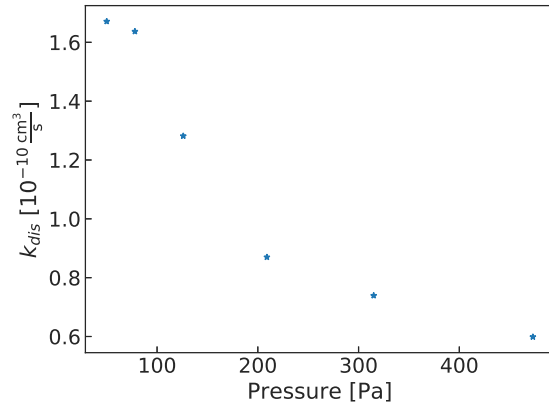


Figure 9. Estimation of dis-alignment coefficient at different measured pressure.

The dis-alignment rate coefficients for most of argon 2p states reported in [15] are a quite different (in range from $1 - 4 \times 10^7 \text{ s}^{-1}$) and additionally with a non uniform

temperature dependency, rendering dis-alignment effect highly important for accurate description of the 2p state densities in a magnetized plasma.

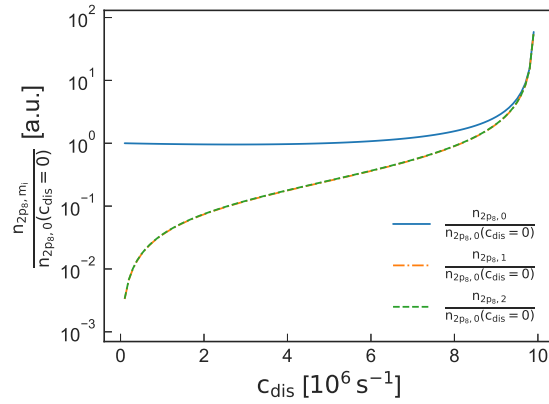


Figure 10. Normalized 2p₈ sub-level densities solved for pumping $m_j = 0$ to $m_i = 0$ transition.

The influence of pressure on sub-state densities in the presence of laser pumping is illustrated in figure 10 where steady state solution for pumping of $m_j = 0$ state by $A_{00}^{842\text{nm}}$ transition is shown. The pressure dependent densities evolution were calculated using constant and low values of 1s₄ and 1s₅ sub-state densities normalized by the value at $c_k = 0$. It is evident that increase of pressure would lead to increase of the population of other not-pumped sub-levels effectively increasing the fluorescence.

The increase of the 2p sub-level densities which are not pumped is a result of a more efficient mixing between the sub-levels until the point when densities within the multiplet are equally distributed having no alignment.

5. Conclusion

A method to evaluate TDLIF measurements accounting for intra-multiplet transitions has been proposed resulting in full quantitative evaluation of the 1s states multiplets involved in the LIF scheme and evaluation of the dis-alignment coefficient for argon. The method was described for the 2p₈ to 1s₄ and 1s₅ scheme but can be easily adopted for other 2p states of argon. As a result a self-consistent evaluation of a alignment by self-absorption could be reconstructed. Such information could further improve an evaluation of a magnetized plasma by optical emission spectroscopy. With the systematic evaluation of dis-alignment for argon 2p levels and quantitative LIF done on various pressures, the densities of all 1s states would be well known, providing basis for further development of an appropriate line branching method for evaluation of a 1s state densities. This properties are making LIF measurements in magnetized plasma as highly efficient tool for quantitative plasma diagnostics while providing basis for further understanding and description of light transport and self-absorption.

Acknowledgments

This work is supported by the Deutsche Forschungsgemeinschaft (DFG).

References

- [1] Zeeman P 1897 *The London, Edinburgh, and Dublin Philosophical Magazine and Journal of Science* **43** 226–239
- [2] Taylor A S, Hyde A R and Batishchev O V 2017 *American Journal of Physics* **85** 565–574
- [3] Fujimoto T and Iwamae A 2008 *Plasma polarization spectroscopy* (Springer)
- [4] Bergert R and Mitic S 2019 *Plasma Sources Science and Technology* **28** 115001 URL [https://doi.org/10.1088%2F1361-6595%2Fab497e](https://doi.org/10.1088/2F1361-6595%2Fab497e)
- [5] Kazantsev S A and Subbotenko A V 1987 *Journal of Physics D: Applied Physics* **20** 741–753 URL <https://doi.org/10.1088%2F0022-3727%2F20%2F6%2F009>
- [6] Fujimoto T and Kazantsev S A 1997 *Plasma physics and controlled fusion* **39** 1267
- [7] Goto M 2003 *Journal of Quantitative Spectroscopy and Radiative Transfer* **76** 331 – 344 ISSN 0022-4073 URL <http://www.sciencedirect.com/science/article/pii/S0022407302000602>
- [8] Iwamae A, Sato T, Horimoto Y, Inoue K, Fujimoto T, Uchida M and Maekawa T 2005 *Plasma physics and controlled fusion* **47** L41
- [9] Teramoto T, Shikama T, Ueda A and Hasuo M 2018 *Applied Physics Letters* **112** 214101 (Preprint <https://doi.org/10.1063/1.5031051>) URL <https://doi.org/10.1063/1.5031051>
- [10] Matsukuma H, Tanaka H, Takaie Y, Shikama T, Bahrim C and Hasuo M 2012 *Journal of the Physical Society of Japan* **81** 114302 URL <https://doi.org/10.1143/JPSJ.81.114302>
- [11] Grandin, JP and Husson, X 1981 *J. Phys. France* **42** 33–37 URL <https://doi.org/10.1051/jphys:0198100420103300>
- [12] Takacs E, Meyer E, Gillaspy J, Roberts J, Chantler C, Hudson L, Deslattes R, Brown C, Laming J, Dubau J *et al.* 1996 *Physical Review A* **54** 1342
- [13] Jacobs V and Filuk A 1999 *Physical Review A* **60** 1975
- [14] Grandin J and Husson X 1978 *Journal de Physique* **39** 933–940
- [15] Grandin J 1973 *Journal de Physique* **34** 403–409
- [16] Kaupe J, Coenen D and Mitic S 2018 *Plasma Sources Science and Technology* **27** 105003
- [17] Mitic S, Kaupe J, Riedl P and Coenen D 2019 *Physics of Plasmas* **26** 073507 (Preprint <https://doi.org/10.1063/1.5092579>) URL <https://doi.org/10.1063/1.5092579>
- [18] Seo M, Nimura M, Hasuo M and Fujimoto T 2003 *Journal of Physics B: Atomic, Molecular and Optical Physics* **36** 1869–1884 URL <https://doi.org/10.1088%2F0953-4075%2F36%2F9%2F316>
- [19] Wakabayashi T, Yamamoto A, Yaneda T, Furutani T, Hishikawa A and Fujimoto T 1998 *Journal of Physics B: Atomic, Molecular and Optical Physics* **31** 341–359 URL <https://doi.org/10.1088%2F0953-4075%2F31%2F2%2F015>